SCIENCE CHINA
Information Sciences

• RESEARCH PAPER •

January 2025, Vol. 68, Iss. 1, 112202:1–112202:17
https://doi.org/10.1007/s11432-023-4053-9

Aperiodically semi-intermittent-based fixed-time stabilization and synchronization of delayed discontinuous inertial neural networks

Guodong ZHANG[1] & Jinde CAO[2*]

[1]*School of Mathematics and Statistics, South-Central Minzu University, Wuhan 430074, China;*
[2]*School of Mathematics, Southeast University, Nanjing 210096, China*

Received 18 July 2023/Revised 18 January 2024/Accepted 29 April 2024/Published online 25 December 2024

Abstract This article concentrates on the fixed-time stabilization (FS) and fixed-time synchronization (FTS) of discontinuous inertial neural networks (DINNs) with distributed delays. Using mathematical induction to a new differential equality, a novel fixed-time stability lemma is constructed. Then, by designing an aperiodically semi-intermittent switching control and combining it with the theory of nonsmooth analysis, some novel criteria on the FS and FTS of DINNs are obtained. Unlike the methods used in most existing studies, the FS and FTS results are structured using the newly proposed fixed-time stability lemma and the nonreduced-order approach, resulting in broader practical applications and strengthening the scientific quality of the derived results. Lastly, numerical simulations and applications proffer the effectiveness of the established FS and FTS criteria.

Keywords inertial neural networks, fixed-time synchronization, semi-intermittent switching control, nonreduced-order approach, fixed-time stabilization

Citation Zhang G D, Cao J D. Aperiodically semi-intermittent-based fixed-time stabilization and synchronization of delayed discontinuous inertial neural networks. Sci China Inf Sci, 2025, 68(1): 112202, https://doi.org/10.1007/s11432-023-4053-9

1 Introduction

As an important aspect of brain-like intelligence, artificial neural networks (ANNs) have become the focus in recent years and have been employed in many studies on brain-like intelligence such as information processing [1,2], forecasting [3], and associative memory [4]. These applications cannot be separated from the dynamic behaviors of ANNs.

Thus, during recent decades, some excellent studies about the dynamic behaviors of ANNs, especially stability and synchronization, have been widely reported [5–13]. For instance, using canonical Bessel-Legendre inequalities, Zhang et al. [6] obtained stability criteria for delayed ANNs. Meanwhile, Kazemy et al. [7] investigated the synchronization of master-slave ANNs under deception attacks via event-triggered control. Li et al. [8] demonstrated the stabilization of delayed ANNs via impulsive control. Cai et al. [9] discussed the exponential synchronization of delayed ANNs with feedback control. Meng et al. [10], Kao and Li [11] studied the stability of fractional-order ANNs. Wang et al. [12] showed the global synchronization of delayed fuzzy memristive ANNs with feedback control. Liu and Ye [13] analyzed the synchronization of memristive ANNs using event-based impulsive control. However, the above studies did not consider inertial items and discontinuous activation functions in their models.

ANNs with inertial item were first constructed and studied by Babcock and Westervelt [14]. In their research, they put inductors into circuits of ANNs, which is called inertial neural networks (INNs). INNs have both biological and engineering backgrounds, where the behaviours of quasi-active membranes in neurons and the squid axon can be simulated by using equivalent-circuits with inductance [15,16], and the unorder searching of memory in neurons can be realized using neural circuits with inductance [17]. Unlike the models expressed with fractional or first-order derivatives of state variables in [5–13], INNs described by second-order derivatives of state variables, which have been proved to be more easily to generate oscillation and chaos behaviors than conventional ANNs. In this regard, previous studies [18–22] showed

* Corresponding author (email: jdcao@seu.edu.cn)

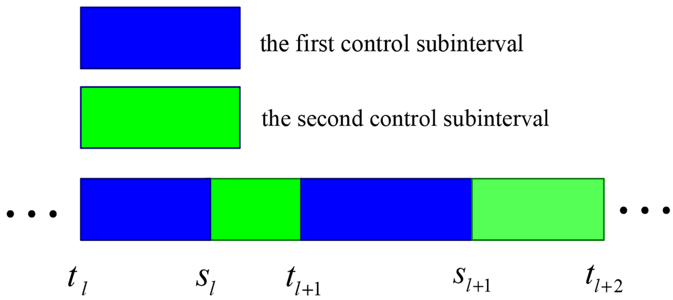

Figure 1 (Color online) Framework of APSIC.

that the synchronization of INNs has some momentous applications in information processing and secure communication. Meanwhile, signal transmission in neural circuits possesses switching characteristics. Discontinuous activations often occur in ANNs [9,23], and ANNs with discontinuous activations are more optimized [23,24]. Thus, Wang et al. [25] and Kong et al. [26] studied discontinuous INNs (DINNs) and found some excellent stability results.

Unfortunately, the stabilization and synchronization of INNs [12–18,26] are all infinite-time, and do not satisfy some actual finite/fixed-time engineering requirements, such as the ANNs-based fixed-time collaborative control of multiple unmanned crafts. Therefore, fixed-time dynamic behaviors of ANNs, especially fixed-time stabilization (FS) and fixed-time synchronization (FTS) have attracted many scholars' attention. Some outstanding studies have been done previously [27–29], and excellent fixed-time results of INNs appeared in previous studies [30–32]. For instance, in 2021, Guo et al. [30] discussed the FTS of complex-valued INNs. Meanwhile, Aouiti et al. [31] studied the FS of delayed fuzzy neutral-type INNs. In another study, Kong et al. [32] investigated the fixed-time stability of DINNs. However, the above studies [25,26,29–32] all used a reduced-order approach to study DINNs. Zhang and Zeng [33] pointed out that the reduced-order approach is unscientific when dealing with discontinuous high-order differential systems. Thus, Zhang and Cao [34] derived the FTS of DINNs using a nonreduced-order approach. Notably, throughout the control processes, the control schemes of earlier studies [29,30,34] were all continuous and had two terms $|e_p^i(t)|$, $|\dot{e}_p^i(t)|$ and $|e_q^j(t)|, |\dot{e}_q^j(t)|\,(0 < i < 1, j > 1)$, where $e_p(t)$ is the pth error state. However, these kinds of controllers are not economical.

As a kind of discontinuous control, aperiodically semi-intermittent switching control (APSIC) (Figure 1) has more economic advantages than continuous controllers [35]. The time span $[t_l, t_{l+1})$ of APSIC is divided into two parts. The systems are activated by a controller in the first intermittent subinterval $[t_l, s_l)$ and are activated by another controller in the second subinterval $[s_l, t_{l+1})$, $t_0 = 0, l = 0, 1, 2, \ldots$. Using proper APSIC, some excellent results in the synchronization of network systems have been obtained [35–37]. In 2019, Zhang et al. [35] achieved the finite-time synchronization of delayed memristive ANNs, whereas Gan et al. [36] obtained the FTS of discontinuous network systems. In 2023, Hu et al. [37] obtained outstanding results on the FS of discontinuous spatiotemporal ANNs via APSIC. Moreover, the APSIC designed in previous studies [36,37] had two terms $|e_p^i(t)|$ and $|e_p^j(t)|\,(0 < i < 1, j > 1)$. In 2021, Li and Wang [38] constructed a new APSIC with only one term $|e_p(t)|^{\omega+\mathrm{sign}(V(t)-1)}\,(1 < \omega < 2)$ and realized the FTS of complex networks. In 2023, based on a previous study [38], Pu and Li [39] studied the FTS on delayed memristive ANNs with such improved APSIC.

However, the above studies [38,39] are all first-order differential systems; until now, there have been no reports on the FS and FTS of DINNs via APSIC, not to mention the use of the nonreduced-order approach and APSIC together to study FS and FTS for DINNs. In fact, there are two challenging problems ahead of us: (1) constructing an APSIC-based fixed-time stability lemma for DINNs and (2) designing an effective APSIC to achieve the FS and FTS of DINNs using the nonreduced-order approach.

Inspired by the above discussion, this study aims to surmount these challenging problems and establish some new results on the FS and FTS for DINNs. The novel points are listed as follows:

(1) A new APSIC-based fixed-time stability lemma is constructed, which is useful for realizing the FS and FTS of DINNs. Moreover, the fixed-time stability lemmas given previously [38,39] are all the special cases of this article.

(2) Unlike the two exponential terms designed in the controllers of earlier studies [29–32,34,36,37], our novel APSIC only has one exponential term in the first intermittent subinterval is established to ensure

the FS and FTS of DINNs.

(3) The ANNs model here has inertial terms, discontinuous activations and distributed delays, which are more general than those in previous studies [27, 28, 30–32, 35–39], where models missed one of the above terms at least. Moreover, the nonreduced-order approach is used here to investigate the FS and FTS of such discontinuous second-order systems, which is more scientific and rigorous.

This paper is divided as follows. Section 2 shows some preliminary studies. The FS and FTS of DINNs are discussed in Section 3. Two simulation examples are given in Section 4. Section 5, shows the conclusion.

Remark 1. In APSIC (Figure 1), if $s_l - t_l = \gimel_1 > 0$, $t_{l+1} - s_l = \gimel_2 > 0$, $l = 0, 1, 2, \ldots$, then, the APSIC is changed into periodically intermittent control considered previously [36, 40]. If $t_{l+1} = s_l, l = 0, 1, 2, \ldots$, the APSIC is turned into continuous control [20, 21, 25–34], where one can see that the APSIC is more general. However, there are no reports based on both APSIC and the nonreduced-order approach to obtain the FS and FTS for DINNs.

Notations. $\boldsymbol{R}^m$ is the m-dimensional Euclidean-space, $\mathcal{Q} = \{1, 2, \ldots, m\}, \mathcal{N} = \{1, 2, \ldots, n\}, \mathcal{P} = \{0, 1, 2, \ldots\}$. For $\forall \digamma = (\digamma_1, \digamma_2, \ldots, \digamma_m)^{\mathrm{T}} \in \mathcal{R}^m$, then, $\|\digamma\|_1 = \sum_{p=1}^m |\digamma_p|$. And $\mathcal{C}([t_0 - \varsigma, t_0], \mathcal{R}^m)$ denotes all continuous-functions $Y(t) : [t_0 - \varsigma, t_0] \mapsto \mathcal{R}^m$, $\mathcal{C}^1(\mathcal{R}^m, [0, +\infty))$ represents all continuous functions with first-order partial-derivatives from $\mathcal{R}^m$ into $[0, +\infty)$. $\varsigma = \max_{1 \leqslant q \leqslant m}\{\varrho_q, \varpi_q\}$. And $K[\wp(t)]$ is the convex closure of $\wp(t), t_0, t \geqslant 0$.

2 Preliminaries

2.1 Model description

Consider a DINN with distributed delays given by

$$\begin{aligned} \frac{\mathrm{d}^2 \mathcal{X}_p(t)}{\mathrm{d}t^2} = & - a_p \mathcal{X}_p(t) - b_p \frac{\mathrm{d}\mathcal{X}_p(t)}{\mathrm{d}t} + \sum_{q=1}^m c_{pq} \Upsilon_q(\mathcal{X}_q(t)) + \sum_{q=1}^m d_{pq} \Upsilon_q(\mathcal{X}_q(t - \varrho_q(t))) \\ & + \sum_{q=1}^m \gamma_{pq} \int_{t - \varpi_q(t)}^t \Upsilon_q(\mathcal{X}_q(s)) \mathrm{d}s, \ t \geqslant 0, \ p \in \mathcal{Q}, \end{aligned} \tag{1}$$

where $\mathcal{X}_p(t)$ is the pth neural state, $\frac{\mathrm{d}^2 \mathcal{X}_p(t)}{\mathrm{d}t^2}$ is an inertial term, $a_p > 0$ and $b_p > 0$ are self-feedback coefficients, $c_{pq}, d_{pq}, \gamma_{pq}$ are connection weights, $\Upsilon_q(\cdot)$ represents discontinuous activation, $\varrho_q(t), \varpi_q(t)$ are time delays that gratify $0 < \varrho_q(t) \leqslant \varrho_q$, and $0 \leqslant \varpi_q(t) \leqslant \varpi_q$. The initial values of (1) are $\mathcal{X}(s) = (\beth_1(s), \beth_2(s), \ldots, \beth_m(s))^{\mathrm{T}}$, $\dot{\mathcal{X}}(s) = (\daleth_1(s), \daleth_2(s), \ldots, \daleth_m(s))^{\mathrm{T}}$, $\mathcal{X}(s), \dot{\mathcal{X}}(s) \in \mathcal{C}([t_0 - \varsigma, t_0], \mathcal{R}^m)$.

In this article, the activation functions $\Upsilon_q(\cdot)\,(q \in \mathcal{Q})$ satisfy the following assumptions.

Assumption $\boldsymbol{H}_1$. Function $\Upsilon_q(\cdot) \in \mathcal{C}(\mathcal{R} \backslash \mathcal{B}_q, \mathcal{R})$, $\mathcal{B}_q$ is a finite set about discontinuous points $\Im_q^\ell$ and has a right-limit $\Upsilon_q(\Im_q^{\ell +})$ and a left-limit $\Upsilon_q(\Im_q^{\ell -}), q \in \mathcal{Q}, \ell \in \mathcal{N}$.

Assumption $\boldsymbol{H}_2$. $\Upsilon_q(0) = 0$. There exists $\Theta_q > 0$ such that $|\Upsilon_q(\cdot)| \leqslant \Theta_q$, and

$$\sup_{x_q \in K[\Upsilon_q(X)],\, y_q \in K[\Upsilon_q(Y)]} |x_q - y_q| \leqslant \Xi_q |X - Y| + \Pi_q,$$

where $\Xi_q \geqslant 0, \Pi_q \geqslant 0, X, Y \in \mathcal{R}$ and $K[\Upsilon_q(X)] = [\min\{\Upsilon_q(X^-), \Upsilon_q(X^+)\}, \max\{\Upsilon_q(X^-), \Upsilon_q(X^+)\}]$, and $K[\Upsilon_q(Y)]$ is similarly defined.

2.2 Definitions of the Filippov solution

Using the theory of differential inclusion [41], one gets the following differential inclusions of DINN (1):

$$\begin{aligned} \frac{\mathrm{d}^2 \mathcal{X}_p(t)}{\mathrm{d}t^2} + b_p \frac{\mathrm{d}\mathcal{X}_p(t)}{\mathrm{d}t} \in & - a_p \mathcal{X}_p(t) + \sum_{q=1}^m c_{pq} K[\Upsilon_q(\mathcal{X}_q(t))] + \sum_{q=1}^m d_{pq} K[\Upsilon_q(\mathcal{X}_q(t - \varrho_q(t)))] \\ & + \sum_{q=1}^m \gamma_{pq} \int_{t - \varpi_q(t)}^t K[\Upsilon_q(\mathcal{X}_q(s))] \mathrm{d}s, \ t \geqslant 0, \ p \in \mathcal{Q}. \end{aligned} \tag{2a}$$

Equivalently, there exists $\Phi_q(t) \in K[\Upsilon_q(\mathcal{X}_q(t))]$; then

$$\frac{\mathrm{d}^2\mathcal{X}_p(t)}{\mathrm{d}t^2} + b_p\frac{\mathrm{d}\mathcal{X}_p(t)}{\mathrm{d}t} = -a_p\mathcal{X}_p(t) + \sum_{q=1}^{m} c_{pq}\Phi_q(t) + \sum_{q=1}^{m} d_{pq}\Phi_q(t-\varrho_q(t)) + \sum_{q=1}^{m}\gamma_{pq}\int_{t-\varpi_q(t)}^{t}\Phi_q(t)\mathrm{d}s,\ p\in\mathcal{Q},\ \text{for a.e. } t\geqslant 0. \tag{2b}$$

Definition 1 ([25])**.** Function $\mathcal{X}(t) = (\mathcal{X}_1(t), \mathcal{X}_2(t), \ldots, \mathcal{X}_m(t))^{\mathrm{T}}$ is named the Filippov solution of DINN (1) with initial values $\mathcal{X}_p(s) = \beth_p(s), \dot{\mathcal{X}}_p(s) = \daleth_p(s), p \in \mathcal{Q}$, and $\beth_p(s), \daleth_p(s) \in \mathcal{C}([t_0-\varsigma, t_0], \mathcal{R})$, if for any compact-interval of $[0, +\infty)$, the absolutely continuous function $\mathcal{X}(t)$ satisfies (2a) or (2b).

Remark 2. Under Assumptions $\boldsymbol{H}_1$ and $\boldsymbol{H}_2$, using the theory of differential inclusion [24,25,41], one gets DINN (1) with a Filippov solution $\mathcal{X}(t)$ at least with initial values $\mathcal{X}_p(s) = \beth_p(s), \dot{\mathcal{X}}_p(s) = \daleth_p(s), p \in \mathcal{Q}$, and $\beth_p(s), \daleth_p(s) \in \mathcal{C}([t_0-\varsigma, t_0], \mathcal{R})$.

2.3 Stabilization model of DINN (1)

In this article, when the DINN is unstable, the stabilization model of DINN (1) is given as follows:

$$\frac{\mathrm{d}^2\mathcal{X}_p(t)}{\mathrm{d}t^2} = -a_p\mathcal{X}_p(t) - b_p\frac{\mathrm{d}\mathcal{X}_p(t)}{\mathrm{d}t} + \sum_{q=1}^{m} c_{pq}\Upsilon_q(\mathcal{X}_q(t)) + \sum_{q=1}^{m} d_{pq}\Upsilon_q(\mathcal{X}_q(t-\varrho_q(t))) + \sum_{q=1}^{m}\gamma_{pq}\int_{t-\varpi_q(t)}^{t}\Upsilon_q(\mathcal{X}_q(s))\mathrm{d}s + u_p(t),\ p\in\mathcal{Q}, \tag{3}$$

where $u_p(t)$ is the APSIC that will be designed later.

2.4 Response system of DINN (1) and the error system

In this article, suppose DINN (1) as the drive system, and its response system is

$$\frac{\mathrm{d}^2\mathcal{Y}_p(t)}{\mathrm{d}t^2} = -a_p\mathcal{Y}_p(t) - b_p\frac{\mathrm{d}\mathcal{Y}_p(t)}{\mathrm{d}t} + \sum_{q=1}^{m} c_{pq}\Upsilon_q(\mathcal{Y}_q(t)) + \sum_{q=1}^{m} d_{pq}\Upsilon_q(\mathcal{Y}_q(t-\varrho_q(t))) + \sum_{q=1}^{m}\gamma_{pq}\int_{t-\varpi_q(t)}^{t}\Upsilon_q(\mathcal{Y}_q(s))\mathrm{d}s + \mathcal{U}_p(t), \tag{4}$$

where $\mathcal{Y}_p(t)$ is the pth state, $\mathcal{U}_p(t)\,(p \in \mathcal{Q})$ is the APSIC that will be shown later, and the rest of the parameters are defined as same as those of DINN (1). The initial values of (4) are $\mathcal{Y}(s) = (\beth_1^*(s), \beth_2^*(s), \ldots, \beth_m^*(s))^{\mathrm{T}}$, $\dot{\mathcal{Y}}(s) = (\daleth_1^*(s), \daleth_2^*(s), \ldots, \daleth_m^*(s))^{\mathrm{T}}$, and $\mathcal{Y}(s), \dot{\mathcal{Y}}(s) \in \mathcal{C}([t_0-\varsigma, t_0], \mathcal{R}^m)$. The definition of the Filippov solution for DINN (4) is the same as above and is thus omitted here.

Let $\mathcal{X}_p(t)$ and $\mathcal{Y}_p(t)\,(p \in \mathcal{Q})$ be two arbitrary Filippov solutions of DINNs (1) and (4) respectively, and the error state $e_p(t) = \mathcal{Y}_p(t) - \mathcal{X}_p(t)$. Then

$$\frac{\mathrm{d}^2 e_p(t)}{\mathrm{d}t^2} = -a_p e_p(t) - b_p\frac{\mathrm{d}e_p(t)}{\mathrm{d}t} + \sum_{q=1}^{m} c_{pq}\Big[\Psi_q(t) - \Phi_q(t)\Big] + \sum_{q=1}^{m} d_{pq}\Big[\Psi_q(t-\varrho_q(t)) - \Phi_q(t-\varrho_q(t))\Big] + \sum_{q=1}^{m}\gamma_{pq}\int_{t-\varpi_q(t)}^{t}\Big[\Psi_q(t) - \Phi_q(t)\Big]\mathrm{d}s + \widetilde{\mathcal{U}}_p(t), \tag{5}$$

where $\Psi_q(t) \in K[\Upsilon_q(\mathcal{Y}_q(t))]$, $\Phi_q(t) \in K[\Upsilon_q(\mathcal{X}_q(t))]$, and $\widetilde{\mathcal{U}}_p(t) \in K[\mathcal{U}_p(t)]$.

2.5 Definition of FTS and lemmas

Definition 2 ([34])**.** DINN (1) are called FS, if there exists a settling-time function $\mathbb{T}(\mathcal{X}(0), \dot{\mathcal{X}}(0)) > 0$, and has a positive constant $\mathbb{T}^s_{\max}$ such that $\mathbb{T}(\mathcal{X}(0), \dot{\mathcal{X}}(0)) \leqslant \mathbb{T}^s_{\max}$ and $\lim_{t\to\mathbb{T}^s_{\max}} \|\widetilde{\mathcal{X}}(t)\|_1 = 0$, where $\mathbb{T}^s_{\max}$ is called the settling time of FS, and $\widetilde{\mathcal{X}}(t) = (\mathcal{X}_1(t), \mathcal{X}_2(t), \ldots, \mathcal{X}_m(t), \dot{\mathcal{X}}_1(t), \dot{\mathcal{X}}_2(t), \ldots, \dot{\mathcal{X}}_m(t))^{\mathrm{T}}, t \geqslant 0$.

Definition 3 ([34])**.** DINNs (1) and (4) are named FTS, and the error system (5) is called fixed-time stable, if the settling-time function $\mathbb{T}(\mathcal{X}(0),\dot{\mathcal{X}}(0),\mathcal{Y}(0),\dot{\mathcal{Y}}(0)) > 0$ and has a positive constant $\mathbb{T}_{\max}$ such that $\mathbb{T}(\mathcal{X}(0),\dot{\mathcal{X}}(0),\mathcal{Y}(0),\dot{\mathcal{Y}}(0)) \leqslant \mathbb{T}_{\max}$ and $\lim_{t\to\mathbb{T}_{\max}} \|\widetilde{e}(t)\|_1 = \lim_{t\to\mathbb{T}_{\max}} \|\widetilde{\mathcal{Y}}(t) - \widetilde{\mathcal{X}}(t)\|_1 = 0$, where $\widetilde{e}(t) = (e_1(t), e_2(t), \ldots, e_m(t), \dot{e}_1(t), \dot{e}_2(t), \ldots, \dot{e}_m(t))^{\mathrm{T}}$, $\widetilde{\mathcal{Y}}(t) = (\mathcal{Y}_1(t), \mathcal{Y}_2(t), \ldots, \mathcal{Y}_m(t), \dot{\mathcal{Y}}_1(t), \dot{\mathcal{Y}}_2(t), \ldots, \dot{\mathcal{Y}}_m(t))^{\mathrm{T}}$, $t \geqslant 0$, and $\mathbb{T}_{\max}$ is named the settling time.

Definition 4 ([36])**.** For APSIC, let $\delta = \limsup_{l\to+\infty} \frac{t_{l+1}-s_l}{t_{l+1}-t_l}$, where $l \in \mathcal{P}$.

Lemma 1 ([42])**.** Vector $\hbar = (\hbar_1, \hbar_2, \ldots, \hbar_m)^{\mathrm{T}} \in \mathcal{R}^m$, for $0 < \imath < \jmath$, then,

$$\left(\sum_{r=1}^{m} |\hbar_r|^{\jmath}\right)^{\frac{1}{\jmath}} \leqslant \left(\sum_{r=1}^{m} |\hbar_r|^{\imath}\right)^{\frac{1}{\imath}} \leqslant m^{\frac{1}{\imath}-\frac{1}{\jmath}} \left(\sum_{r=1}^{m} |\hbar_r|^{\jmath}\right)^{\frac{1}{\jmath}}.$$

Lemma 2. Let the radially unbounded regular function $\mathbb{V}(\cdot) \in \mathcal{C}(\boldsymbol{R}^{2m}, [0,+\infty))$, $L(t) = 0 \Leftrightarrow \mathbb{V}(L(t)) = 0$, and follow with almost all solutions of (3) or (5). If for $t \in [0,+\infty)$, $\mathbb{V}(t)$ satisfies

$$\frac{\mathrm{d}\mathbb{V}(t)}{\mathrm{d}t} \leqslant \begin{cases} \alpha\mathbb{V}(t) - \beta\mathbb{V}^{\kappa}(t) - \xi, & t_l \leqslant t < s_l, \\ 0, & s_l \leqslant t < t_{l+1},\ l \in \mathcal{P}, \end{cases} \tag{6}$$

where $\kappa = \omega + \mathrm{sign}(\mathbb{V}(t) - 1)$, $1 < \omega < 2$, $\beta > 0$, $\alpha < \beta$, $\xi > 0$, then, system (3) or (5) is fixed-time stable, and DINNs (1) and (4) realize FTS at settling time $\mathbb{T}_{\max}$, which is

$$\mathbb{T}_{\max} = \begin{cases} \dfrac{1}{(1-\delta)}\left(\dfrac{1}{(2-\omega)(\beta+\xi-\alpha)} + \dfrac{1}{(\beta-\alpha)\omega}\right), & \alpha > 0, \\ \dfrac{1}{(1-\delta)}\left(\dfrac{1}{(2-\omega)(\beta+\xi)} + \dfrac{1}{\beta\omega}\right), & \alpha \leqslant 0. \end{cases} \tag{7}$$

Proof. From (6), we can easily get that $\dot{\mathbb{V}}(t) \leqslant 0\,(t \geqslant 0)$ always holds. Two cases should be considered.

(C1) If $\alpha > 0$, for (6), the following are the two cases due to $\mathbb{V}(t)$.

• When $\mathbb{V}(t) < 1$, one has $\mathbb{V}^{\kappa}(t) = \mathbb{V}^{\omega-1}(t)$, $\mathbb{V}(t) \leqslant \mathbb{V}^{\omega-1}(t)$ and $-\xi \leqslant -\xi\mathbb{V}^{\omega-1}(t)$. Then, Eq. (6) changes into

$$\frac{\mathrm{d}\mathbb{V}(t)}{\mathrm{d}t} \leqslant \begin{cases} -(\beta+\xi-\alpha)\mathbb{V}^{\omega-1}(t), & t_l \leqslant t < s_l, \\ 0, & s_l \leqslant t < t_{l+1},\ l \in \mathcal{P}. \end{cases} \tag{8}$$

For $t \in [0, s_0)$, let $\Gamma_0(t) = \Omega(t) - \Delta_0$ and $\Omega(t) = \mathbb{V}^{2-\omega}(t) + (\beta+\xi-\alpha)(2-\omega)t, \Delta_0 = \mathbb{V}^{2-\omega}(0)$. Through simple computation, one gets $\Gamma_0(0) = 0, \dot{\Gamma}_0(t) \leqslant 0$. Then, for $\forall\, t \in [0, s_0)$, $\Omega(t) \leqslant \Delta_0$.

For $t \in [s_0, t_1)$, let $\Gamma_0^*(t) = \Omega(t) - (\beta+\xi-\alpha)(2-\omega)(t-s_0) - \Delta_0$, because $\Omega(s_0) \leqslant \Delta_0$ and $\dot{\Gamma}_0^*(t) \leqslant 0$. Then, $\Omega(t) \leqslant (\beta+\xi-\alpha)(2-\omega)(t-s_0) + \Delta_0$.

Using mathematical induction similar to that of a previous study [35], for $t_l \leqslant t < s_l$, one obtains the following inequality:

$$\Omega(t) \leqslant \Delta_0 + (\beta+\xi-\alpha)(2-\omega)\sum_{i=1}^{l}(t_i - s_{i-1}). \tag{9}$$

For $s_l \leqslant t < t_{l+1}$, one obtains another inequality:

$$\Omega(t) \leqslant \Delta_0 + (\beta+\xi-\alpha)(2-\omega)\left(\sum_{i=1}^{l}(t_i - s_{i-1}) + t - s_l\right). \tag{10}$$

From Definition 4, we know $0 \leqslant \delta < 1$. From (9) and (10) and by using processes similar to those of a previous study [35], one has

$$\Omega(t) \leqslant \Delta_0 + (\beta+\xi-\alpha)(2-\omega)\delta t,\ t \in [0,+\infty). \tag{11}$$

Then, for $t \in [0,+\infty)$, one gets

$$\mathbb{V}^{2-\omega}(t) \leqslant \Delta_0 - (\beta+\xi-\alpha)(2-\omega)(1-\delta)t. \tag{12}$$

Due to $\Delta_0 \leqslant 1$, from (12), we have the settling time is

$$\mathcal{T}_1 = \frac{1}{(\beta+\xi-\alpha)(2-\omega)(1-\delta)}. \tag{13}$$

- When $\mathbb{V}(t) > 1$, one knows $\mathbb{V}^{\kappa}(t) = \mathbb{V}^{\omega+1}(t)$ and $\mathbb{V}(t) \leqslant \mathbb{V}^{\omega+1}(t)$. Then, Eq. (6) turns into

$$\frac{\mathrm{d}\mathbb{V}(t)}{\mathrm{d}t} \leqslant \begin{cases} -(\beta-\alpha)\mathbb{V}^{\omega+1}(t), & t_l \leqslant t < s_l, \\ 0, & s_l \leqslant t < t_{l+1},\ l \in \mathcal{P}. \end{cases} \tag{14}$$

For $t \in [0, s_0)$, let $\overline{\Gamma}_0(t) = \overline{\Omega}(t) - \overline{\Delta}_0$, and $\overline{\Omega}(t) = \mathbb{V}^{-\omega}(t) - (\beta-\alpha)\omega t, \overline{\Delta}_0 = \mathbb{V}^{-\omega}(0)$. Through simple computation, one has $\overline{\Gamma}_0(0) = 0, \dot{\overline{\Gamma}}_0(t) \geqslant 0$. Then, for $\forall\, t \in [0, s_0)$, $\overline{\Omega}(t) \geqslant \overline{\Delta}_0$.

For $t \in [s_0, t_1)$, let $\overline{\Gamma}_0^*(t) = \overline{\Omega}(t) + (\beta-\alpha)\omega(t-s_0) - \overline{\Delta}_0$, because $\overline{\Omega}(s_0) \geqslant \overline{\Delta}_0$ and $\dot{\overline{\Gamma}}^*{}_0(t) \geqslant 0$. Then, $\overline{\Omega}(t) \geqslant \overline{\Delta}_0 - (\beta-\alpha)\omega(t-s_0)$.

Using processes similar to those above, for $t_l \leqslant t < s_l$, the following inequality holds:

$$\overline{\Omega}(t) \geqslant \overline{\Delta}_0 - (\beta-\alpha)\omega\sum_{i=1}^{l}(t_i - s_{i-1}). \tag{15}$$

For $s_l \leqslant t < t_{l+1}$, another inequality holds

$$\overline{\Omega}(t) \geqslant \overline{\Delta}_0 - (\beta-\alpha)\omega\left(\sum_{i=1}^{l}(t_i - s_{i-1}) + t - s_l\right). \tag{16}$$

From (15) and Definition 4, one gets

$$\begin{aligned}\overline{\Omega}(t) &\geqslant \overline{\Delta}_0 - (\beta-\alpha)\omega\sum_{i=1}^{l}\frac{t_i - s_{i-1}}{t_i - t_{i-1}}(t_i - t_{i-1}) \\ &\geqslant \overline{\Delta}_0 - (\beta-\alpha)\omega\delta t,\ t_l \leqslant t < s_l.\end{aligned} \tag{17}$$

From (16) and Definition 4, one has

$$\begin{aligned}\overline{\Omega}(t) &\geqslant \overline{\Delta}_0 - (\beta-\alpha)\omega\left(\sum_{i=1}^{l}(t_i - s_{i-1}) + t - s_l\right) \\ &\geqslant \overline{\Delta}_0 - (\beta-\alpha)\omega\left(\sum_{i=1}^{l}\frac{t_i - s_{i-1}}{t_i - t_{i-1}}(t_i - t_{i-1}) + \frac{t - s_1}{t - t_l}(t - t_l)\right) \\ &\geqslant \overline{\Delta}_0 - (\beta-\alpha)\omega\delta t,\ s_l \leqslant t < t_{l+1}.\end{aligned} \tag{18}$$

From (17) and (18), one derives

$$\overline{\Omega}(t) \geqslant \overline{\Delta}_0 - (\beta-\alpha)\omega\delta t,\ t \in [0, +\infty). \tag{19}$$

Then, for $t \in [0, +\infty)$, one obtains

$$\mathbb{V}^{-\omega}(t) \geqslant \overline{\Delta}_0 + (\beta-\alpha)\omega(1-\delta)t. \tag{20}$$

Because of $\overline{\Delta}_0 < 1$ and from (20), one can get $\mathbb{V}(t) \to 1$ when $t \to \mathcal{T}_2$, where $\mathcal{T}_2 = \frac{1}{(\beta-\alpha)\omega(1-\delta)}$. Because $\mathbb{V}(t)$ is monotonously decreasing, $\mathbb{V}(t)$ continues to decrease over 1 until it reaches 0 at settling time $\mathbb{T}^1 = \mathcal{T}_1 + \mathcal{T}_2$; that is,

$$\mathbb{T}^1 = \frac{1}{(1-\delta)}\left(\frac{1}{(2-\omega)(\beta+\xi-\alpha)} + \frac{1}{(\beta-\alpha)\omega}\right). \tag{21}$$

(C2) If $\alpha \leqslant 0$, for (6), there are two cases due to $\mathbb{V}(t)$.

• When $\mathbb{V}(t) < 1$, one has $\mathbb{V}^{\kappa}(t) = \mathbb{V}^{\omega-1}(t)$ and $-\xi \leqslant -\xi\mathbb{V}^{\omega-1}(t)$. Then, Eq. (6) changes into

$$\frac{\mathrm{d}\mathbb{V}(t)}{\mathrm{d}t} \leqslant \begin{cases} l - (\beta+\xi)\mathbb{V}^{\omega-1}(t), & t_l \leqslant t < s_l, \\ 0, & s_l \leqslant t < t_{l+1},\ l \in \mathcal{P}. \end{cases} \tag{22}$$

From (22) and using processes similar to those in (C1) one gets $\mathbb{V}(t) \to 0$ when $t \to \mathcal{T}_1^* = \frac{1}{(\beta+\xi)(2-\omega)(1-\delta)}$.

• When $\mathbb{V}(t) > 1$, one has $\mathbb{V}^{\kappa}(t) = \mathbb{V}^{\omega+1}(t)$. Then, Eq. (6) changes into

$$\frac{\mathrm{d}\mathbb{V}(t)}{\mathrm{d}t} \leqslant \begin{cases} -\beta\mathbb{V}^{\omega+1}(t), & t_l \leqslant t < s_l, \\ 0, & s_l \leqslant t < t_{l+1},\ l \in \mathcal{P}. \end{cases} \tag{23}$$

From (23) and using processes similar to those of (C1), one gets $\mathbb{V}(t) \to 1$ when $t \to \mathcal{T}_2^* = \frac{1}{\beta\omega(1-\delta)}$. Then, $\mathbb{V}(t)$ continues to decrease over 1 until it reaches 0 at settling time $\mathbb{T}^2 = \mathcal{T}_1^* + \mathcal{T}_2^*$; that is,

$$\mathbb{T}^2 = \frac{1}{(1-\delta)}\left(\frac{1}{(2-\omega)(\beta+\xi)} + \frac{1}{\beta\omega}\right). \tag{24}$$

Now, from (21) and (24), one has Lemma 2 hold. This ends the proof.

Remark 3. Time delays cannot avoid in neural circuits. When discussing the FS or FTS for delayed neural systems, feedback functions with time delays are usually scaled to a constant by the bounded condition, which often leads to a positive constant ξ appears in the right of (6). However, most of the previous studies completely abandoned such positive constants in the results of their FS and FTS. If $0 < \kappa < 1, \alpha = \xi = 0$, (6) of this paper changes into the inequality of a previous study [35]. However, such research [35] only showed the finite-time stable results and its neural systems were only first-order differential systems which were also without discontinuous activations. Meanwhile, previous results on fixed-time stability of [37] need the condition $\int_{t_0}^{+\infty} \alpha^+ \mathrm{d}s < +\infty\ (\alpha^+ = \max\{\alpha, 0\})$. However, Lemma 2 of this article does not need such a restrictive condition. In fact, if $\alpha > 0$, one has $\int_{t_0}^{+\infty} \alpha\ \mathrm{d}s \to +\infty$. When this case occurs, the results of [37] lose their meaning. If $\alpha = \xi = 0$, (6) of this paper changes into the inequality of previous studies [38, 39]. Thus, such results [38, 39] are all the special cases of Lemma 2 in this article. Therefore, Lemma 2 obtained here has made substantial progress on FS and FTS for continuous or discontinuous differential systems via APSIC.

3 Main results

3.1 FS of DINN (1)

The APSIC $u_p(t)\,(p \in \mathcal{Q})$ in the stabilization model (3) of DINN (1) is given as follows:

$$u_p(t) = \begin{cases} -\zeta_p\mathcal{X}_p(t) - \mu_p\dot{\mathcal{X}}_p(t) - \mathrm{sign}(\dot{\mathcal{X}}_p(t))(\lambda_p|\mathcal{X}_p^{\kappa}(t)| + \chi_p|\dot{\mathcal{X}}_p^{\kappa}(t)| + \nu_p), & t_l \leqslant t < s_l, \\ -(\vartheta_p\mathcal{X}_p(t) + \nu_p)\mathrm{sign}(\dot{\mathcal{X}}_p(t)) - \mu_p\dot{\mathcal{X}}_p(t), & s_l \leqslant t < t_{l+1},\ l \in \mathcal{P}, \end{cases} \tag{25}$$

where $\zeta_p, \mu_p, \lambda_p, \chi_p, \vartheta_p, \nu_p$ are all nonnegative constants and $\kappa = \omega + \mathrm{sign}(\mathbb{V}(t)-1), 1 < \omega < 2$. Moreover, $\widetilde{u}_p(t)$ is

$$\widetilde{u}_p(t) = \begin{cases} -\zeta_p\mathcal{X}_p(t) - \mu_p\dot{\mathcal{X}}_p(t) - \varphi_p(t)(\lambda_p|\mathcal{X}_p^{\kappa}(t)| + \chi_p|\dot{\mathcal{X}}_p^{\kappa}(t)| + \nu_p), & \text{for } t_l \leqslant t < s_l, \\ -(\vartheta_p\mathcal{X}_p(t) + \nu_p)\varphi_p(t) - \mu_p\dot{\mathcal{X}}_p(t), & \text{for } s_l \leqslant t < t_{l+1},\ p \in \mathcal{Q}, l \in \mathcal{P}, \end{cases} \tag{26}$$

where $\varphi_p(t) \in K[\text{sign}(\dot{\mathcal{X}}_p(t))]$. Then, the control model (3) turns into

$$\frac{\mathrm{d}^2\mathcal{X}_p(t)}{\mathrm{d}t^2} = \begin{cases} -(a_p+\zeta_p)\mathcal{X}_p(t) - (b_p+\mu_p)\dfrac{\mathrm{d}\mathcal{X}_p(t)}{\mathrm{d}t} + \sum\limits_{q=1}^{m} c_{pq}\Phi_q(t) + \sum\limits_{q=1}^{m} d_{pq}\Phi_q(t-\varrho_q(t)) \\ +\sum\limits_{q=1}^{m}\gamma_{pq}\displaystyle\int_{t-\varpi_q(t)}^{t}\Phi_q(t)\mathrm{d}s - \varphi_p(t)(\lambda_p|\mathcal{X}_p^{\kappa}(t)| + \chi_p|\dot{\mathcal{X}}_p^{\kappa}(t)| + \nu_p), \\ \text{for } t_l \leqslant t < s_l, \\ -(a_p+\vartheta_p\varphi_p(t))\mathcal{X}_p(t) - (b_p+\mu_p)\dfrac{\mathrm{d}\mathcal{X}_p(t)}{\mathrm{d}t} + \sum\limits_{q=1}^{m} c_{pq}\Phi_q(t) + \sum\limits_{q=1}^{m} d_{pq}\Phi_q(t-\varrho_q(t)) \\ +\sum\limits_{q=1}^{m}\gamma_{pq}\displaystyle\int_{t-\varpi_q(t)}^{t}\Phi_q(t)\mathrm{d}s - \varphi_p(t)\nu_p, \text{ for } s_l \leqslant t < t_{l+1},\ l \in \mathcal{P}. \end{cases} \tag{27}$$

To show the FS results clearly, the following notations are given at first:

$$\alpha = \max_{1\leqslant p\leqslant m}\left\{1-b_p-\mu_p, a_p+\zeta_p+\sum_{q=1}^{m}|c_{qp}|\Xi_p\right\}, \tag{28}$$

$$\beta_1 = \min_{1\leqslant p\leqslant m}\{\lambda_p,\chi_p\},\ \beta=\beta_1\cdot(2m)^{-\omega},\ \xi=\sum_{p=1}^{m}\xi_p, \tag{29}$$

$$\xi_p = \nu_p - \sum_{q=1}^{m}\Big(|c_{pq}|\Pi_q + (|d_{pq}|+|\gamma_{pq}|\varpi_q)\Theta_q\Big),$$

$$1-b_p-\mu_p<0,\ a_p+\sum_{q=1}^{m}|c_{qp}|\Xi_p<\vartheta_p,\ \xi_p>0. \tag{30}$$

Theorem 1. If Assumptions $\boldsymbol{H}_1, \boldsymbol{H}_2$, $\alpha<\beta$ and (30) hold, then, DINN (1) can obtain FS with APSIC (25) at settling time $\mathbb{T}_{\max}$, which is given in (7).

Proof. The nonnegative function is

$$\mathbb{V}(t) = \sum_{p=1}^{m}\left(\left|\frac{\mathrm{d}\mathcal{X}_p(t)}{\mathrm{d}t}\right| + |\mathcal{X}_p(t)|\right). \tag{31}$$

For $t_l \leqslant t < s_l\,(l\in\mathcal{P})$, using the properties of C-regular function in [43] and along the solutions of (3), then the derivative of $\mathbb{V}(t)$ is

$$\begin{aligned}\frac{\mathrm{d}\mathbb{V}(t)}{\mathrm{d}t} =& \sum_{p=1}^{m}\left\{\frac{\mathrm{d}\mathcal{X}_p(t)}{\mathrm{d}t}\psi_p(t) + \frac{\mathrm{d}^2\mathcal{X}_p(t)}{\mathrm{d}t^2}\varphi_p(t)\right\} \\ =& \sum_{p=1}^{m}\left\{\frac{\mathrm{d}\mathcal{X}_p(t)}{\mathrm{d}t}\psi_p(t) + \varphi_p(t)\Bigg(-(a_p+\zeta_p)\mathcal{X}_p(t) - (b_p+\mu_p)\frac{\mathrm{d}\mathcal{X}_p(t)}{\mathrm{d}t}\right. \\ &+\sum_{q=1}^{m}c_{pq}\Phi_q(t) + \sum_{q=1}^{m}d_{pq}\Phi_q(t-\varrho_q(t)) + \sum_{q=1}^{m}\gamma_{pq}\int_{t-\varpi_q(t)}^{t}\Phi_q(t)\mathrm{d}s\Bigg) \\ &\left.-\varphi_p(t)(\lambda_p|\mathcal{X}_p^{\kappa}(t)| + \chi_p|\dot{\mathcal{X}}_p^{\kappa}(t)| + \nu_p)\right\},\end{aligned} \tag{32}$$

where $\psi_p(t) \in K[\text{sign}(\mathcal{X}_p(t))]$. From (32), one gets

$$\frac{\mathrm{d}\mathbb{V}(t)}{\mathrm{d}t} \leqslant \sum_{p=1}^{m}\left\{(1-b_p-\mu_p)\left|\frac{\mathrm{d}\mathcal{X}_p(t)}{\mathrm{d}t}\right| + (a_p+\zeta_p)|\mathcal{X}_p(t)| + \sum_{q=1}^{m}|c_{pq}||\Phi_q(t)|\right.$$

$$+\sum_{q=1}^{m}|d_{pq}||\Phi_q(t-\varrho_q(t))|+\sum_{q=1}^{m}\left|\gamma_{pq}\int_{t-\varpi_q(t)}^{t}\Phi_q(t)\mathrm{d}s\right|$$
$$-\left(\lambda_p|\mathcal{X}_p^{\kappa}(t)|+\chi_p|\dot{\mathcal{X}}_p^{\kappa}(t)|+\nu_p\right)\Bigg\}. \tag{33}$$

Under $\boldsymbol{H}_1$ and $\boldsymbol{H}_2$, one has the following estimation of (33):

$$\begin{aligned}\frac{\mathrm{d}\mathbb{V}(t)}{\mathrm{d}t}\leqslant&\sum_{p=1}^{m}\Bigg\{(1-b_p-\mu_p)\left|\frac{\mathrm{d}\mathcal{X}_p(t)}{\mathrm{d}t}\right|+(a_p+\zeta_p)|\mathcal{X}_p(t)|\\&+\sum_{q=1}^{m}|c_{pq}|(\Xi_q|\mathcal{X}_q(t)|+\Pi_q)+\sum_{q=1}^{m}|d_{pq}|\Theta_q+\sum_{q=1}^{m}|\gamma_{pq}|\varpi_q\Theta_q\\&-\left(\lambda_p|\mathcal{X}_p^{\kappa}(t)|+\chi_p|\dot{\mathcal{X}}_p^{\kappa}(t)|+\nu_p\right)\Bigg\}\\\leqslant&\sum_{p=1}^{m}\Bigg\{(1-b_p-\mu_p)\left|\frac{\mathrm{d}\mathcal{X}_p(t)}{\mathrm{d}t}\right|+\left(a_p+\zeta_p+\sum_{q=1}^{m}|c_{qp}|\Xi_p\right)|\mathcal{X}_p(t)|-\lambda_p|\mathcal{X}_p^{\kappa}(t)|\\&-\chi_p|\dot{\mathcal{X}}_p^{\kappa}(t)|-\left[\nu_p-\sum_{q=1}^{m}\left(|c_{pq}|\Pi_q+(|d_{pq}|+|\gamma_{pq}|\varpi_q)\Theta_q\right)\right]\Bigg\}.\end{aligned} \tag{34}$$

Using Lemma 1, when $\mathbb{V}(t)<1, \kappa=\omega-1$, because $0<\omega-1<1$, then,

$$\begin{aligned}-\sum_{p=1}^{m}(\lambda_p|\mathcal{X}_p^{\kappa}(t)|+\chi_p|\dot{\mathcal{X}}_p^{\kappa}(t)|)\leqslant&-\beta_1\sum_{p=1}^{m}\left(|\mathcal{X}_p^{\omega-1}(t)|+|\dot{\mathcal{X}}_p^{\omega-1}(t)|\right)\\\leqslant&-\beta_1\left(\sum_{p=1}^{m}(|\mathcal{X}_p(t)|+|\dot{\mathcal{X}}_p(t)|)\right)^{\omega-1}\\=&-\beta_1\mathbb{V}^{\kappa}(t).\end{aligned} \tag{35}$$

When $\mathbb{V}(t)>1, \kappa=\omega+1$, because $1<\omega+1$, then,

$$\begin{aligned}-\sum_{p=1}^{m}(\lambda_p|\mathcal{X}_p^{\kappa}(t)|+\chi_p|\dot{\mathcal{X}}_p^{\kappa}(t)|)\leqslant&-\beta_1\sum_{p=1}^{m}\left(|\mathcal{X}_p^{\omega+1}(t)|+|\dot{\mathcal{X}}_p^{\omega+1}(t)|\right)\\\leqslant&-\frac{\beta_1}{(2m)^{\omega}}\left(\sum_{p=1}^{m}(|\mathcal{X}_p(t)|+|\dot{\mathcal{X}}_p(t)|)\right)^{\omega+1}\\=&-\beta_1(2m)^{-\omega}\mathbb{V}^{\kappa}(t).\end{aligned} \tag{36}$$

Therefore, from (29), (35) and (36), one knows, for $t_l\leqslant t<s_l\,(l\in\mathcal{P})$,

$$-\sum_{p=1}^{m}(\lambda_p|\mathcal{X}_p^{\kappa}(t)|+\chi_p|\dot{\mathcal{X}}_p^{\kappa}(t)|)\leqslant-\beta\mathbb{V}^{\kappa}(t). \tag{37}$$

Using (28), (29), (34) and (37), one obtains

$$\frac{\mathrm{d}\mathbb{V}(t)}{\mathrm{d}t}\leqslant\alpha\mathbb{V}(t)-\beta\mathbb{V}^{\kappa}(t)-\xi,\ t_l\leqslant t<s_l\,(l\in\mathcal{P}). \tag{38}$$

Now, for $s_l\leqslant t<t_{l+1}\,(l\in\mathcal{P})$, from (30) and (34), we get

$$\frac{\mathrm{d}\mathbb{V}(t)}{\mathrm{d}t}\leqslant\sum_{p=1}^{m}\Bigg\{(1-b_p-\mu_p)\left|\frac{\mathrm{d}\mathcal{X}_p(t)}{\mathrm{d}t}\right|-\left(\vartheta_p-a_p-\sum_{q=1}^{m}|c_{qp}|\Xi_p\right)|\mathcal{X}_p(t)|$$

$$- \left[\nu_p - \sum_{q=1}^{m} \Big(|c_{pq}|\Pi_q + (|d_{pq}| + |\gamma_{pq}|\varpi_q)\Theta_q \Big) \right] \Bigg\}$$
$$\leqslant 0. \tag{39}$$

From (38) and (39), one can find that Eq. (6) holds. Then, using Lemma 2, Eq. (3) is fixed-time stable; thus, DINN (1) can obtain FS with APSIC (25) at settling time $\mathbb{T}_{\max}$. This ends the proof.

3.2 FTS of DINNs (1) and (4)

The APSIC $\mathcal{U}_p(t)\,(p \in \mathcal{Q})$ in response DINN (4) is given as follows:

$$\mathcal{U}_p(t) = \begin{cases} -\zeta_p^* e_p(t) - \mu_p^* \dot{e}_p(t) - \mathrm{sign}(\dot{e}_p(t))(\lambda_p^* |e_p^\kappa(t)| + \chi_p^* |\dot{e}_p^\kappa(t)| + \nu_p^*), & t_l \leqslant t < s_l, \\ -(\vartheta_p^* e_p(t) + \nu_p^*)\mathrm{sign}(\dot{e}_p(t)) - \mu_p^* \dot{e}_p(t), & s_l \leqslant t < t_{l+1},\ l \in \mathcal{P}, \end{cases} \tag{40}$$

where $\zeta_p, \mu_p, \lambda_p, \chi_p, \vartheta_p, \nu_p$ are all nonnegative constants and $\kappa = \omega + \mathrm{sign}(\mathbb{V}(t) - 1), 1 < \omega < 2$. Moreover, $\widetilde{\mathcal{U}}_p(t)$ of error system (5) is

$$\widetilde{\mathcal{U}}_p(t) = \begin{cases} -\zeta_p^* e_p(t) - \mu_p^* \dot{e}_p(t) - \varphi_p(t)(\lambda_p^* |e_p^\kappa(t)| + \chi_p^* |\dot{e}_p^\kappa(t)| + \nu_p^*), & \text{for } t_l \leqslant t < s_l, \\ -(\vartheta_p^* e_p(t) + \nu_p^*)\varphi_p(t) - \mu_p^* \dot{e}_p(t), & \text{for } s_l \leqslant t < t_{l+1},\ p \in \mathcal{Q}, l \in \mathcal{P}. \end{cases} \tag{41}$$

Then, error system (5) turns into be

$$\frac{\mathrm{d}^2 e_p(t)}{\mathrm{d}t^2} = \begin{cases} -(a_p + \zeta_p^*)e_p(t) - (b_p + \mu_p^*)\dfrac{\mathrm{d}e_p(t)}{\mathrm{d}t} + \displaystyle\sum_{q=1}^{m} c_{pq}\Big[\Psi_q(t) - \Phi_q(t)\Big] \\ + \displaystyle\sum_{q=1}^{m} d_{pq}\Big[\Psi_q(t-\varrho_q(t)) - \Phi_q(t-\varrho_q(t))\Big] + \displaystyle\sum_{q=1}^{m} \gamma_{pq} \int_{t-\varpi_q(t)}^{t} \Big[\Psi_q(t) \\ - \Phi_q(t)\Big]\mathrm{d}s - \varphi_p(t)(\lambda_p^* |e_p^\kappa(t)| + \chi_p^* |\dot{e}_p^\kappa(t)| + \nu_p^*), \text{ for } t_l \leqslant t < s_l, \\ -(a_p + \vartheta_p^* \varphi_p(t))e_p(t) - (b_p + \mu_p^*)\dfrac{\mathrm{d}e_p(t)}{\mathrm{d}t} + \displaystyle\sum_{q=1}^{m} c_{pq}\Big[\Psi_q(t) - \Phi_q(t)\Big] \\ + \displaystyle\sum_{q=1}^{m} d_{pq} \times \Big[\Psi_q(t-\varrho_q(t)) - \Phi_q(t-\varrho_q(t))\Big] \\ + \displaystyle\sum_{q=1}^{m} \gamma_{pq} \int_{t-\varpi_q(t)}^{t} \Big[\Psi_q(t) - \Phi_q(t)\Big]\mathrm{d}s - \varphi_p(t)\nu_p^*, \text{ for } s_l \leqslant t < t_{l+1},\ l \in \mathcal{P}. \end{cases} \tag{42}$$

To show the FTS results clearly, the following notations are given first:

$$\alpha^* = \max_{1 \leqslant p \leqslant m} \left\{ 1 - b_p - \mu_p^*, a_p + \zeta_p^* + \sum_{q=1}^{m} |c_{qp}|\Xi_p \right\}, \tag{43}$$

$$\beta_1^* = \min_{1 \leqslant p \leqslant m} \{\lambda_p^*, \chi_p^*\},\ \beta^* = \beta_1^* \cdot (2m)^{-\omega},\ \xi^* = \sum_{p=1}^{m} \xi_p^*, \tag{44}$$

$$\xi_p^* = \nu_p^* - \sum_{q=1}^{m} \Big(|c_{pq}|\Pi_q + 2(|d_{pq}| + |\gamma_{pq}|\varpi_q)\Theta_q \Big),$$

$$1 - b_p - \mu_p^* < 0,\ a_p + \sum_{q=1}^{m} |c_{qp}|\Xi_p < \vartheta_p^*,\ \xi_p^* > 0. \tag{45}$$

Theorem 2. If Assumptions $\boldsymbol{H}_1, \boldsymbol{H}_2$, $\alpha^* < \beta^*$ and Eq. (45) hold, then, DINNs (1) and (4) obtain FTS with APSIC (40) at settling time $\mathbb{T}^*_{\max}$, which is

$$\mathbb{T}^*_{\max} = \begin{cases} \dfrac{1}{(1-\delta)}\left(\dfrac{1}{(2-\omega)(\beta^*+\xi^*-\alpha^*)} + \dfrac{1}{(\beta^*-\alpha^*)\omega}\right), & \alpha^* > 0, \\ \dfrac{1}{(1-\delta)}\left(\dfrac{1}{(2-\omega)(\beta^*+\xi^*)} + \dfrac{1}{\beta^*\omega}\right), & \alpha^* \leqslant 0. \end{cases} \tag{46}$$

Proof. The nonnegative function is

$$\mathbb{V}(t) = \sum_{p=1}^{m}\left(\left|\frac{\mathrm{d}e_p(t)}{\mathrm{d}t}\right| + |e_p(t)|\right). \tag{47}$$

For $t_l \leqslant t < s_l \, (l \in \mathcal{P})$, using the properties of the C-regular function in [43] and along the solutions of (42), then the derivative of $\mathbb{V}(t)$ is

$$\begin{aligned} \frac{\mathrm{d}\mathbb{V}(t)}{\mathrm{d}t} =& \sum_{p=1}^{m}\left\{\frac{\mathrm{d}e_p(t)}{\mathrm{d}t}\psi_p(t) + \frac{\mathrm{d}^2 e_p(t)}{\mathrm{d}t^2}\varphi_p(t)\right\} \\ =& \sum_{p=1}^{m}\left\{\frac{\mathrm{d}e_p(t)}{\mathrm{d}t}\psi_p(t) + \varphi_p(t)\Bigg(-(a_p+\zeta_p^*)e_p(t) - (b_p+\mu_p^*)\frac{\mathrm{d}e_p(t)}{\mathrm{d}t}\right. \\ &+ \sum_{q=1}^{m} c_{pq}\Big[\Psi_q(t) - \Phi_q(t)\Big] + \sum_{q=1}^{m} d_{pq}\Big[\Psi_q(t-\varrho_q(t)) - \Phi_q(t-\varrho_q(t))\Big] \\ &\left. + \sum_{q=1}^{m}\gamma_{pq}\int_{t-\varpi_q(t)}^{t}\Big[\Psi_q(t) - \Phi_q(t)\Big]\mathrm{d}s - \varphi_p(t)(\lambda_p^*|e_p^\kappa(t)| + \chi_p^*|\dot{e}_p^\kappa(t)| + \nu_p^*)\right\}. \end{aligned} \tag{48}$$

From (48), one gets

$$\begin{aligned} \frac{\mathrm{d}\mathbb{V}(t)}{\mathrm{d}t} \leqslant& \sum_{p=1}^{m}\left\{(1-b_p-\mu_p^*)\left|\frac{\mathrm{d}e_p(t)}{\mathrm{d}t}\right| + (a_p+\zeta_p^*)|e_p(t)| + \sum_{q=1}^{m}|c_{pq}||\Psi_q(t)-\Phi_q(t)|\right. \\ &+ \sum_{q=1}^{m}|d_{pq}||\Psi_q(t-\varrho_q(t)) - \Phi_q(t-\varrho_q(t))| + \sum_{q=1}^{m}\left|\gamma_{pq}\int_{t-\varpi_q(t)}^{t}\Big[\Psi_q(t)-\Phi_q(t)\Big]\mathrm{d}s\right| \\ &\left. - \Big(\lambda_p^*|e_p^\kappa(t)| + \chi_p^*|\dot{e}_p^\kappa(t)| + \nu_p^*\Big)\right\}. \end{aligned} \tag{49}$$

Under $\boldsymbol{H}_1$ and $\boldsymbol{H}_2$, one has the following estimation of (49):

$$\begin{aligned} \frac{\mathrm{d}\mathbb{V}(t)}{\mathrm{d}t} \leqslant& \sum_{p=1}^{m}\left\{(1-b_p-\mu_p^*)\left|\frac{\mathrm{d}e_p(t)}{\mathrm{d}t}\right| + (a_p+\zeta_p^*)|e_p(t)| + \sum_{q=1}^{m}|c_{pq}|(\Xi_q|e_q(t)| + \Pi_q)\right. \\ &\left. + 2\sum_{q=1}^{m}|d_{pq}|\Theta_q + 2\sum_{q=1}^{m}|\gamma_{pq}|\varpi_q\Theta_q - \Big(\lambda_p^*|e_p^\kappa(t)| + \chi_p^*|\dot{e}_p^\kappa(t)| + \nu_p^*\Big)\right\} \\ \leqslant& \sum_{p=1}^{m}\left\{(1-b_p-\mu_p^*)\left|\frac{\mathrm{d}e_p(t)}{\mathrm{d}t}\right| + \left(a_p+\zeta_p^* + \sum_{q=1}^{m}|c_{qp}|\Xi_p\right)|e_p(t)|\right. \\ &\left. - \lambda_p^*|e_p^\kappa(t)| - \chi_p^*|\dot{e}_p^\kappa(t)| - \left[\nu_p^* - \sum_{q=1}^{m}\Big(|c_{pq}|\Pi_q + 2(|d_{pq}| + |\gamma_{pq}|\varpi_q)\Theta_q\Big)\right]\right\}. \end{aligned} \tag{50}$$

Using a proof similar to that of Theorem 1, one has

$$\frac{\mathrm{d}\mathbb{V}(t)}{\mathrm{d}t} \leqslant \alpha^*\mathbb{V}(t) - \beta^*\mathbb{V}^\kappa(t) - \xi^*, \; t_l \leqslant t < s_l. \tag{51}$$

Now, for $s_l \leqslant t < t_{l+1}$ $(l \in \mathcal{P})$, from (45) and (50), one gets

$$\begin{aligned}\frac{\mathrm{d}\mathbb{V}(t)}{\mathrm{d}t} \leqslant &\sum_{p=1}^{m}\left\{(1-b_p-\mu_p^*)\left|\frac{\mathrm{d}e_p(t)}{\mathrm{d}t}\right| - \left(\vartheta_p^* - a_p - \sum_{q=1}^{m}|c_{qp}|\Xi_p\right)|e_p(t)|\right. \\ &\left. - \left[\nu_p^* - \sum_{q=1}^{m}\Big(|c_{pq}|\Pi_q + 2(|d_{pq}| + |\gamma_{pq}|\varpi_q)\Theta_q\Big)\right]\right\} \\ \leqslant &0. \end{aligned} \tag{52}$$

From (51) and (52), one can find that Eq. (6) holds. Then, by using Lemma 2, Eq. (42) is fixed-time stable; thus, DINNs (1) and (4) obtain FTS with APSIC (40) at settling time $\mathbb{T}^*_{\max}$. This ends the proof.

Remark 4. Previous studies [5–7, 9, 19–22] only discussed the asymptotic synchronization of ANNs. Herein, meanwhile, the FTS of neural systems is established. If the systems (1) and (4) are without inertial terms, which turns into the first-order differential systems widely studied previously [9, 12, 13, 27, 39], the main results of this article are also held for such first-order neural systems. Therefore, the FTS results in this paper are more comprehensive and abundant. Although the FTS of INNs have been discussed previously [29–32, 34], their control schemes were continuous. Unlike these previous studies, we designed a proper APSIC to obtain the FTS of DINNs (1) and (4) using the newly proposed Lemma 2, which does not always require the right of (6) to have exponential terms at all times.

Remark 5. The INNs investigated previously [19, 20, 26, 29, 32] were all discontinuous with right-hand sides. Using the reduced-order method and continuous control schemes, these papers showed some meaningful results on the synchronization or FTS for such INNs. After using the reduced-order method, the stability criteria of INNs usually included parameters unrelated to the original system. If the parameters were inappropriately selected, the stability frameworks became meaningless. In addition, previous authors [33] pointed out that the reduced-order method is not rigorous enough for studying discontinuous high-order differential systems. Using the provided Lemma 2 and by constructing proper APSIC (25) and (40), this article completely improved the above studies in terms of both the scientific quality of the analytical method and the control scheme. In addition, Lemma 2 can be used to study FS or FTS for other complex systems, such as complex-valued networks, memristive-based state-switched networks, and so on. This article shows us some necessary preparations to further investigate the above issues.

4 Numerical simulations

To demonstrate the effectiveness of our results and control scheme, the following numerical simulations are enumerated.

Example 1. A two-dimensional DINN is

$$\begin{cases}\dfrac{\mathrm{d}^2\mathcal{X}_1(t)}{\mathrm{d}t^2} = -a_1\mathcal{X}_1(t) - b_1\dfrac{\mathrm{d}\mathcal{X}_1(t)}{\mathrm{d}t} + \displaystyle\sum_{q=1}^{2}c_{1q}\Upsilon_q(\mathcal{X}_q(t)) + \sum_{q=1}^{2}d_{1q}\Upsilon_q(\mathcal{X}_q(t-\varrho_q(t))) \\ \qquad\qquad + \displaystyle\sum_{q=1}^{2}\gamma_{1q}\int_{t-\varpi_q(t)}^{t}\Upsilon_q(\mathcal{X}_q(s))\mathrm{d}s, \\ \dfrac{\mathrm{d}^2\mathcal{X}_2(t)}{\mathrm{d}t^2} = -a_2\mathcal{X}_2(t) - b_2\dfrac{\mathrm{d}\mathcal{X}_2(t)}{\mathrm{d}t} + \displaystyle\sum_{q=1}^{2}c_{2q}\Upsilon_q(\mathcal{X}_q(t)) + \sum_{q=1}^{2}d_{2q}\Upsilon_q(\mathcal{X}_q(t-\varrho_q(t))) \\ \qquad\qquad + \displaystyle\sum_{q=1}^{2}\gamma_{2q}\int_{t-\varpi_q(t)}^{t}\Upsilon_q(\mathcal{X}_q(s))\mathrm{d}s,\end{cases} \tag{53}$$

where $\varrho_q(t) = \varpi_q(t) = \frac{\exp\{t\}}{1+\exp\{t\}}, q = 1, 2$, and

$$\Upsilon_q(\mathcal{X}_q(t)) = \begin{cases}\tanh(\mathcal{X}_q(t)), & \mathcal{X}_q(t) \leqslant 1, \\ \tanh(\mathcal{X}_q(t)) + 0.2, & \mathcal{X}_q(t) > 1.\end{cases} \tag{54}$$

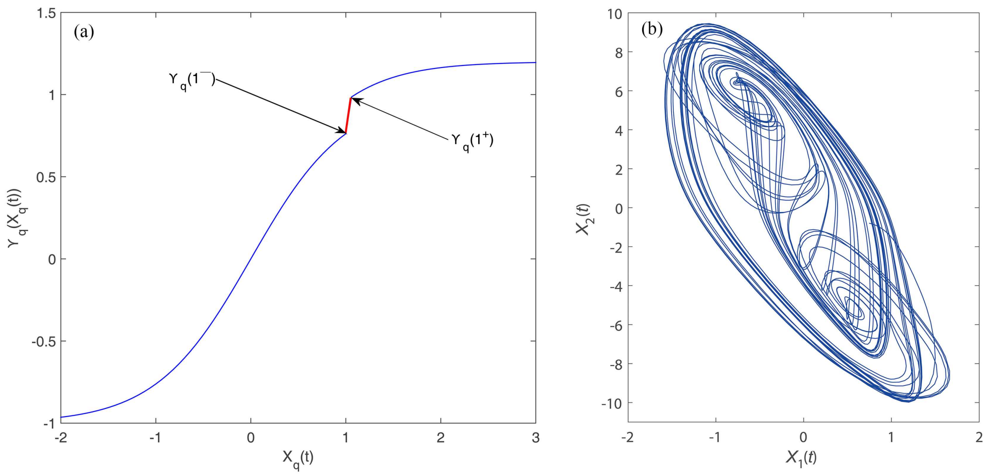

Figure 2 (Color online) (a) Discontinuous activation function of DINN (53); (b) phase diagram of chaotic attractors for DINN (53).

Table 1 Parameter values of DINN (53).

	a_1	b_1	c_{11}	c_{12}	d_{11}	d_{12}	γ_{11}	γ_{12}
Value	0.78	0.68	1.85	−0.1	−1.4	−0.1	−0.02	−0.01
	a_2	b_2	c_{21}	c_{22}	d_{21}	d_{22}	γ_{21}	γ_{22}
Value	1.3	1.4	−8.5	3	−0.5	−1	−0.05	0.1

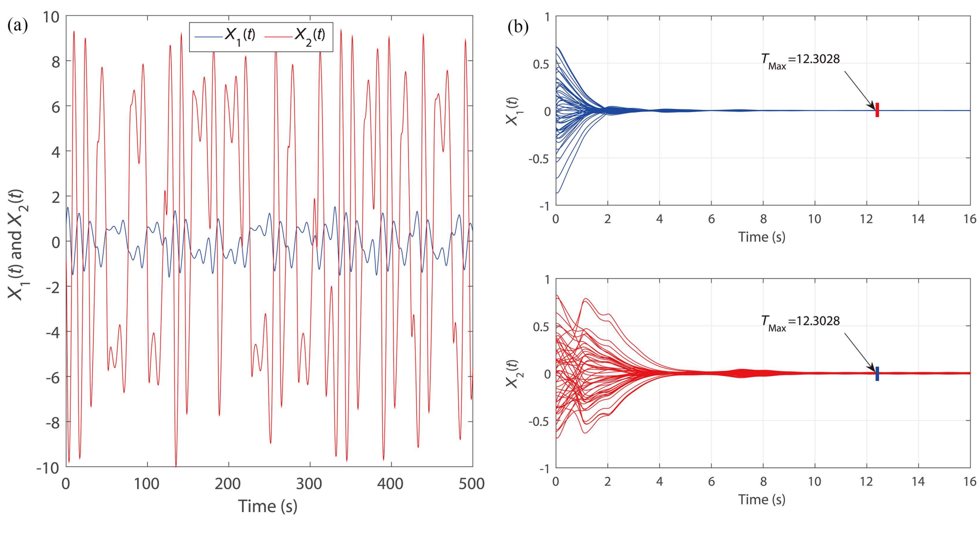

Figure 3 (Color online) (a) States $\mathcal{X}_1(t)$ and $\mathcal{X}_2(t)$ of DINN (53) without control; (b) state trajectories $\mathcal{X}_1(t)$ and $\mathcal{X}_2(t)$ of DINN (53) with APSIC (25).

The discontinuous activation function (54) is given in Figure 2(a). The values of the other parameters are shown in Table 1. By choosing the initial values $\beth_1(s) = 0.75, \daleth_1(s) = 0.7, \beth_2(s) = -0.8, \daleth_2(s) = -0.7, \forall s \in [-1, 0)$, then DINN (53) has chaotic attractors, as shown in Figure 2(b), and Figure 3(a) shows the time responses of $\mathcal{X}_1(t)$ and $\mathcal{X}_2(t)$ without control input.

From (53) and (54), one has $\Xi_1 = \Xi_2 = 1, \Pi_1 = \Pi_2 = 0.2, \Theta_1 = \Theta_2 = 1.2, \varpi_1 = \varpi_2 = 1$, and $m = 2$. To stabilize DINN (53), we chose $t_l = l, s_l = l + 0.6$, and $\omega = 1.2$, and the other parameters of APSIC (25) are given in Table 2. Through simple computation, we get $\delta = 0.4, \alpha = 20, \beta = 20.1969, \xi = 0.2$. From (7), one has $\mathbb{T}_{\max} = 12.3028$. Now, all conditions of Theorem 1 hold; thus, DINN (53) gets FS at settling time $\mathbb{T}_{\max} = 12.3028$. When 50 initial values were chosen randomly, Figure 3(b) shows that the state trajectories $\mathcal{X}_1(t)$ and $\mathcal{X}_2(t)$ of DINN (53) obtained FS with APSIC (25).

Now, we show the FTS between DINN (53) and its response system using APSIC (40). The response

Table 2 Parameter values of APSIC (25).

	ζ_1	μ_1	λ_1	χ_1	ν_1	ϑ_1
Value	8.87	0.33	106.6	106.6	2.326	12
	ζ_2	μ_2	λ_2	χ_2	ν_2	ϑ_2
Value	8.87	0.2	106.6	106.6	4.38	4.5

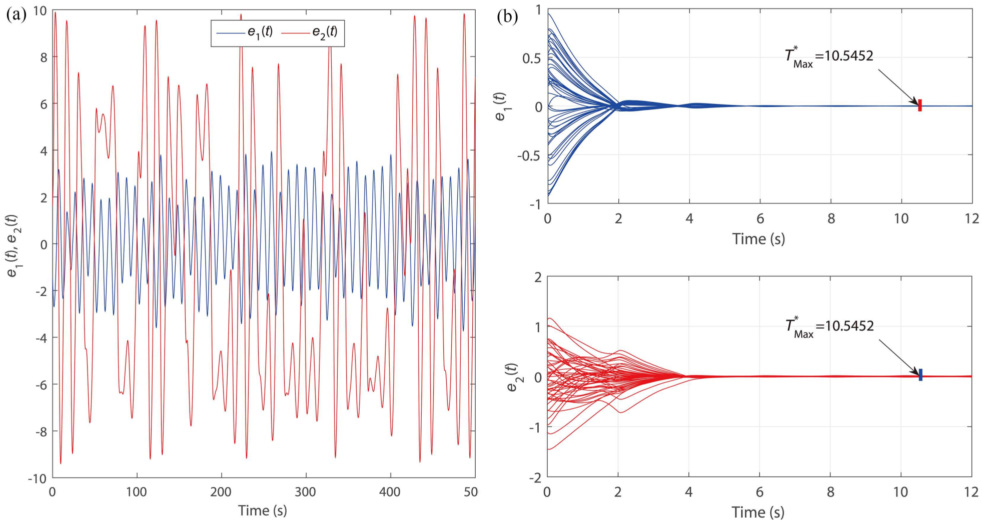

Figure 4 (Color online) (a) Error states $e_1(t)$ and $e_2(t)$ between DINNs (53) and (55) without APSIC (40); (b) error states $e_1(t)$ and $e_2(t)$ between DINNs (53) and (55) with APSIC (40).

system for DINN (53) is

$$\begin{cases} \frac{\mathrm{d}^2\mathcal{Y}_1(t)}{\mathrm{d}t^2} = -a_1\mathcal{Y}_1(t) - b_1\frac{\mathrm{d}\mathcal{Y}_1(t)}{\mathrm{d}t} + \sum_{q=1}^{2} c_{1q}\Upsilon_q(\mathcal{Y}_q(t)) + \sum_{q=1}^{2} d_{1q}\Upsilon_q(\mathcal{Y}_q(t-\varrho_q(t))) \\ \qquad + \sum_{q=1}^{2}\gamma_{1q}\int_{t-\varpi_q(t)}^{t}\Upsilon_q(\mathcal{Y}_q(s))\mathrm{d}s + \mathcal{U}_1(t), \\ \frac{\mathrm{d}^2\mathcal{Y}_2(t)}{\mathrm{d}t^2} = -a_2\mathcal{Y}_2(t) - b_2\frac{\mathrm{d}\mathcal{Y}_2(t)}{\mathrm{d}t} + \sum_{q=1}^{2} c_{2q}\Upsilon_q(\mathcal{Y}_q(t)) + \sum_{q=1}^{2} d_{2q}\Upsilon_q(\mathcal{Y}_q(t-\varrho_q(t))) \\ \qquad + \sum_{q=1}^{2}\gamma_{2q}\int_{t-\varpi_q(t)}^{t}\Upsilon_q(\mathcal{Y}_q(s))\mathrm{d}s + \mathcal{U}_2(t), \end{cases} \tag{55}$$

where the parameters are given as in DINN (53). The initial values of (55) are $\beth_1^*(s) = -0.75, \daleth_1^*(s) = -0.7, \beth_2^*(s) = 0.8$, and $\daleth_2^*(s) = 0.7$, $\forall s \in [-1, 0)$. The error states $e_1(t)$ and $e_2(t)$ between DINNs (53) and (55) without APSIC (40) are displayed in Figure 4(a) and are unstable.

To get the FTS for DINNs (53) and (55), for APSIC (40), we chose $t_l = 2l, s_l = 2(l + 0.7), \zeta_1^* = \zeta_2^* = \zeta_1, \mu_1^* = \mu_1, \mu_2^* = \mu_2, \lambda_1^* = \lambda_2^* = \chi_1^* = \chi_2^* = \lambda_1, \nu_1^* = 4.162, \nu_2^* = 6.36, \vartheta_1^* = \vartheta_1, \vartheta_2^* = \vartheta_2$, and $\omega = 1.2$. Through simple computation, we get $\delta = 0.3, \alpha^* = 20, \beta^* = 20.1969$, and $\xi^* = 0.2$. From (7), one has $\mathbb{T}^*_{\max} = 10.5452$. Now, all conditions of Theorem 2 hold; thus, DINNs (53) and (55) obtain FTS at settling time $\mathbb{T}^*_{\max} = 10.5452$. When 50 initial values were chosen randomly, Figure 4(b) shows that the error trajectories $e_1(t)$ and $e_2(t)$ of DINNs (53) and (55) obtained FTS with APSIC (40). The synchronization curves $\mathcal{X}_1(t), \mathcal{Y}_1(t)$ and $\mathcal{X}_2(t), \mathcal{Y}_2(t)$ between DINNs (53) and (55) are shown in Figures 5(a) and (b), respectively.

Remark 6. For convenience, in Figures 2(b), 3(a) and (b), 5(a) and (b), we used the marks X and Y to stand for the marks $\mathcal{X}$ and $\mathcal{Y}$, respectively.

Remark 7. From the numerical simulations in Example 1, one can clearly find that Lemma 2 and APSIC (25) and (40) constructed in this article were very effective in obtaining FS and FTS for DINNs.

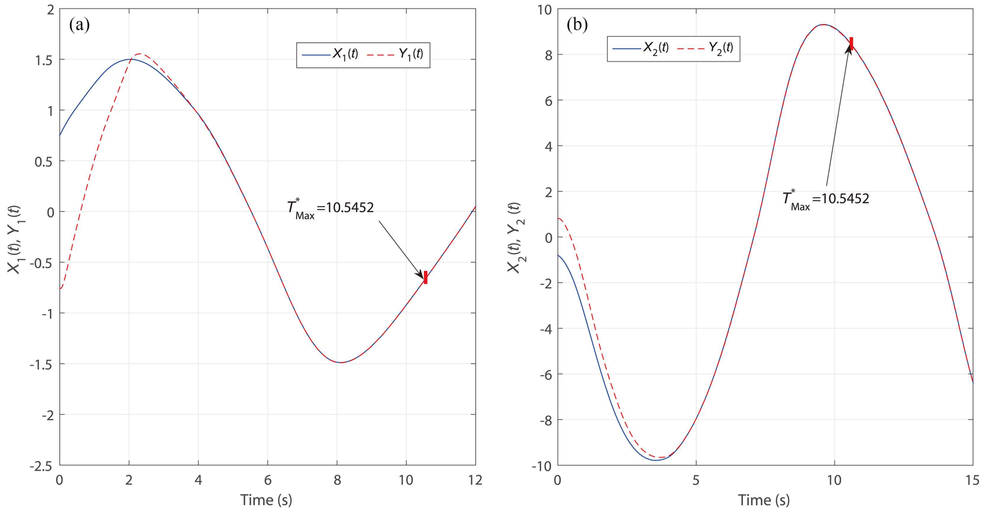

Figure 5 (Color online) Synchronization curves of (a) $\mathcal{X}_1(t)$ and $\mathcal{Y}_1(t)$, (b) $\mathcal{X}_2(t)$ and $\mathcal{Y}_2(t)$.

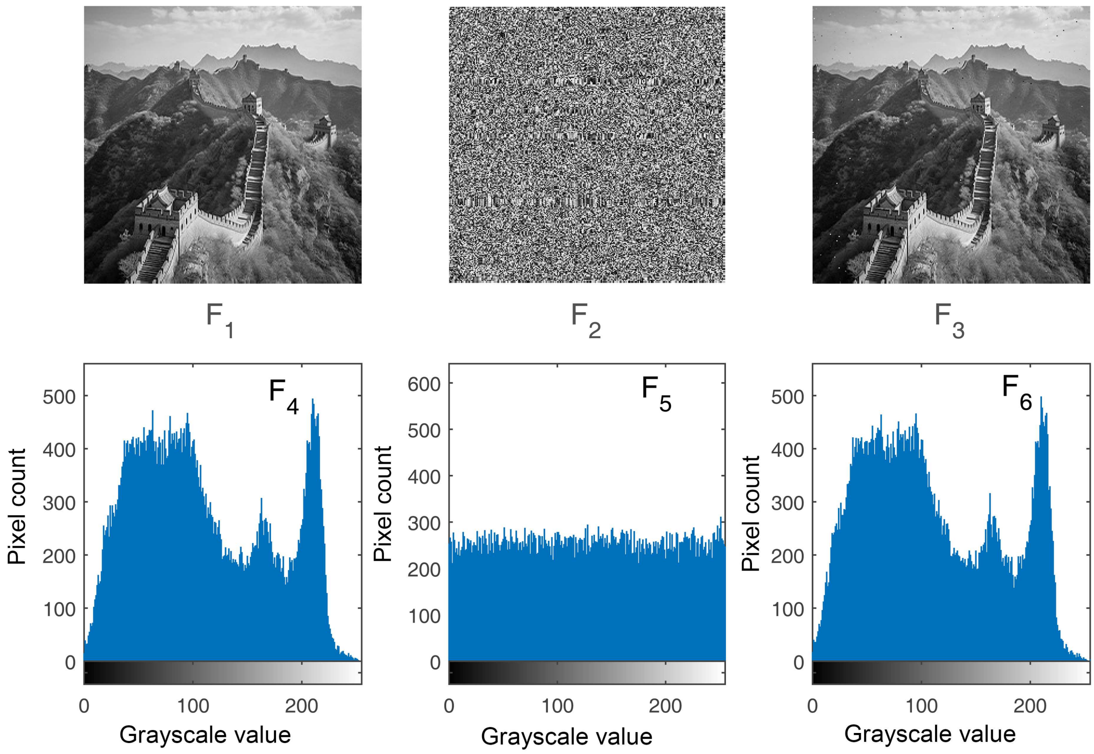

Figure 6 (Color online) Result of chaos-synchronization between DINNs (53) and (55) is used in image encryption and decryption.

We believe that the proposed method and Lemma 2 can also be used to deal with FS and FTS for other general differential systems.

Example 2. Here, we show an application of FTS in image encryption and decryption. On the basis of the FTS in Example 1 and [34], such an application is given in Figure 6, where the original image is F_1 and the encrypted and decrypted images are F_2 and F_3, respectively. F_4–F_6 are the histograms of F_1–F_3, respectively.

Remark 8. Table 3 [18–22, 25, 26, 29–34] compares the novel points of this article and some recent studies from six aspects (i.e., the inertial term, discontinuous activation, fixed-time results, nonreduced approach, APSIC, and Lemma 2). $\times$ means not existing and $\surd$ implies existence. Table 3 shows that this article is the first one to use Lemma 2, APSIC, and the nonreduced approach to obtain the FTS of DINNs.

Table 3 Comparisons with some recent earlier studies.

Refs.	Inertial term	Discontinuous	FTS	Non-reduced method	APSIC	Lemma 2
[18–20]	√	√	×	×	×	×
[21, 22, 33]	√	√	×	√	×	×
[25, 26]	√	√	×	×	×	×
[30, 31]	√	×	√	×	×	×
[29, 32]	√	√	√	×	×	×
[34]	√	√	√	√	×	×
This paper	√	√	√	√	√	√

5 Conclusion

The FS and FTS of DINNs were discussed in this article. Unlike most previous studies that used the reduced-order method and continuous control schemes to study DINNs, a new Lemma 2 on fixed-time stability for differential systems was proposed. Moreover, some novel criteria were given to ensure the FS and FTS of the considered DINNs using effective APSIC and the nonreduced-order method, which completely improved previous studies [18–20, 25, 26, 29–32] in terms of the scientific quality of both the analytical method and control scheme.

The results of this article offer substantial progress on FS and FTS for continuous or discontinuous differential systems using APSIC. Moreover, the analytical methods proposed in this article further expand and enrich theoretical research tools on nonlinear dynamic systems.

Acknowledgements This work was supported by National Natural Science Foundation of China (Grant No. 61976228), National Key Research and Development Project of China (Grant No. 2020YFA0714301), and Fundamental Research Funds of the Central Universities of South-Central Minzu University (Grant No. CZQ24020).

References

1 Sun W, Chen S, Huang L, et al. Deep convolutional neural network compression via coupled tensor decomposition. IEEE J Sel Top Signal Process, 2021, 15: 603–616
2 Zhu D, Chen Y, Zhao D, et al. Multiscale brain-like neural network for saliency prediction on omnidirectional images. IEEE Trans Cogn Dev Syst, 2022, 14: 507–518
3 Sangiorgio M, Dercole F, Guariso G. Forecasting of noisy chaotic systems with deep neural networks. Chaos Soliton Fract, 2021, 153: 111570
4 Shen Y, Zhu S, Liu X, et al. Multistability and associative memory of neural networks with Morita-like activation functions. Neural Netw, 2021, 142: 162–170
5 Zhang X M, Han Q L, Ge X, et al. An overview of recent developments in Lyapunov-Krasovskii functionals and stability criteria for recurrent neural networks with time-varying delays. Neurocomputing, 2018, 313: 392–401
6 Zhang X M, Han Q L, Zeng Z. Hierarchical type stability criteria for delayed neural networks via canonical Bessel-Legendre inequalities. IEEE Trans Cybern, 2018, 48: 1660–1671
7 Kazemy A, Lam J, Zhang X M. Event-triggered output feedback synchronization of master-slave neural networks under deception attacks. IEEE Trans Neural Netw Learn Syst, 2022, 33: 952–961
8 Li X D, Song S J, Wu J H. Impulsive control of unstable neural networks with unbounded time-varying delays. Sci China Inf Sci, 2018, 61: 012203
9 Cai Z, Huang L, Zhang L. New exponential synchronization criteria for time-varying delayed neural networks with discontinuous activations. Neural Netw, 2015, 65: 105–114
10 Meng X, Kao Y G, Karimi H R, et al. Global Mittag-Leffler stability for fractional-order coupled systems on network without strong connectedness. Sci China Inf Sci, 2020, 63: 132201
11 Kao Y G, Li H. Asymptotic multistability and local S-asymptotic ω-periodicity for the nonautonomous fractional-order neural networks with impulses. Sci China Inf Sci, 2021, 64: 112207
12 Wang L, He H, Zeng Z. Global synchronization of fuzzy memristive neural networks with discrete and distributed delays. IEEE Trans Fuzzy Syst, 2020, 28: 2022–2034
13 Liu D, Ye D. Exponential synchronization of memristive delayed neural networks via event-based impulsive control method. J Franklin Inst, 2020, 357: 4437–4457
14 Babcock K L, Westervelt R M. Stability and dynamics of simple electronic neural networks with added inertia. Phys D-Nonlinear Phenomena, 1986, 23: 464–469
15 Ashmore J, Attwell D. Models for electrical tuning in hair cells. Proc Royal Soc London B Biolog Sci, 1985, 226: 325–344
16 Angelaki D E, Correia M J. Models of membrane resonance in pigeon semicircular canal type II hair cells. Biol Cybern, 1991, 65: 1–10
17 Tani J. Model-based learning for mobile robot navigation from the dynamical systems perspective. IEEE Trans Syst Man Cybern B, 1996, 26: 421–436
18 Xiao Q, Huang T, Zeng Z. Passivity and passification of fuzzy memristive inertial neural networks on time scales. IEEE Trans Fuzzy Syst, 2016, 26: 3342–3355
19 Prakash M, Balasubramaniam P, Lakshmanan S. Synchronization of Markovian jumping inertial neural networks and its applications in image encryption. Neural Netw, 2016, 83: 86–93
20 Li N, Zheng W X. Synchronization criteria for inertial memristor-based neural networks with linear coupling. Neural Netw, 2018, 106: 260–270
21 Zhang T, Jian J. New results on synchronization for second-order fuzzy memristive neural networks with time-varying and infinite distributed delays. Knowl-Based Syst, 2021, 230: 107397
22 Zhang G, Zeng Z, Ning D. Novel results on synchronization for a class of switched inertial neural networks with distributed delays. Inf Sci, 2020, 511: 114–126
23 Tank D, Hopfield J. Simple 'neural' optimization networks: an A/D converter, signal decision circuit, and a linear programming circuit. IEEE Trans Circ Syst, 1986, 33: 533–541

24 Forti M, Grazzini M, Nistri P, et al. Generalized Lyapunov approach for convergence of neural networks with discontinuous or non-Lipschitz activations. Phys D-Nonlinear Phenomena, 2006, 214: 88–99
25 Wang L, Zeng Z, Zong X, et al. Finite-time stabilization of memristor-based inertial neural networks with discontinuous activations and distributed delays. J Franklin Inst, 2019, 356: 3628–3643
26 Kong F, Ren Y, Sakthivel R. New criteria on periodicity and stabilization of discontinuous uncertain inertial Cohen-Grossberg neural networks with proportional delays. Chaos Soliton Fract, 2021, 150: 111148
27 Hu C, Yu J, Chen Z, et al. Fixed-time stability of dynamical systems and fixed-time synchronization of coupled discontinuous neural networks. Neural Netw, 2017, 89: 74–83
28 Gan Q, Li L, Yang J, et al. Improved results on fixed-/preassigned-time synchronization for memristive complex-valued neural networks. IEEE Trans Neural Netw Learn Syst, 2022, 33: 5542–5556
29 Chen C, Li L, Peng H, et al. Fixed-time synchronization of inertial memristor-based neural networks with discrete delay. Neural Netw, 2019, 109: 81–89
30 Guo R, Lu J, Li Y, et al. Fixed-time synchronization of inertial complex-valued neural networks with time delays. Nonlinear Dyn, 2021, 105: 1643–1656
31 Aouiti C, Hui Q, Jallouli H, et al. Fixed-time stabilization of fuzzy neutral-type inertial neural networks with time-varying delay. Fuzzy Sets Syst, 2021, 411: 48–67
32 Kong F, Zhu Q, Huang T. New fixed-time stability lemmas and applications to the discontinuous fuzzy inertial neural networks. IEEE Trans Fuzzy Syst, 2021, 29: 3711–3722
33 Zhang G, Zeng Z. Stabilization of second-order memristive neural networks with mixed time delays via nonreduced order. IEEE Trans Neural Netw Learn Syst, 2020, 31: 700–706
34 Zhang G D, Cao J D. New results on fixed/predefined-time synchronization of delayed fuzzy inertial discontinuous neural networks: non-reduced order approach. Appl Math Comput, 2023, 440: 127671
35 Zhang S, Yang Y, Sui X, et al. Finite-time synchronization of memristive neural networks with parameter uncertainties via aperiodically intermittent adjustment. Phys A-Stat Mech its Appl, 2019, 534: 122258
36 Gan Q, Xiao F, Qin Y, et al. Fixed-time cluster synchronization of discontinuous directed community networks via periodically or aperiodically switching control. IEEE Access, 2019, 7: 83306–83318
37 Hu X F, Wang L M, Zhang C K, et al. Fixed-time stabilization of discontinuous spatiotemporal neural networks with time-varying coefficients via aperiodically switching control. Sci China Inf Sci, 2023, 66: 152204
38 Li N, Wang P. Synchronization of complex networks with simple fixed-time semi-intermittent control. In: Proceedings of Chinese Control Conference, 2021. 546–551
39 Pu H, Li F. Fixed-time projective synchronization of delayed memristive neural networks via aperiodically semi-intermittent switching control. ISA Trans, 2023, 133: 302–316
40 Yu J, Hu C, Jiang H, et al. Exponential lag synchronization for delayed fuzzy cellular neural networks via periodically intermittent control. Math Comput Simul, 2012, 82: 895–908
41 Filippov A F. Differential Equations with Discontinuous Right-hand Sides. Dordrecht: Kluwer, 1988
42 Hardy G, Littlewood J, Pólya G. Inequalities. 2nd ed. Cambridge: Cambridge University Press, 1952
43 Clarke F H, Ledyaev Y S, Stem R J, et al. Nonsmooth Analysis and Control Theory. New York: Springer, 1998